System Identification and Structural Control on the JPL Phase B Testbed

Jet Propulsion Laboratory
California Institute of Technology
Pasadena, CA

Cheng-Chih Chu
John F. O'Brien
Boris J. Lurie

Introduction

The primary objective of NASA's CSI program at JPL is to develop and demonstrate the CSI technology required to achieve high precision structural stability on large complex optical class spacecraft. The focus mission for this work is an orbiting interferometer telescope [1]. Toward the realization of such a mission, a series of evolutionary testbed structures are being constructed. The JPL's CSI Phase B testbed is the second structure constructed in this series which is designed to study the pathlength control problem of the optical train of a stellar interferometer telescope mounted on a large flexible structure. A detailed description of this testbed can be found in [2].

This paper describes our efforts in the first phase of active structural control experiments of Phase B testbed using the active control approach where a single piezoelectric active member is used as an actuation device and the measurements include both colocated and noncolocated sensors. Our goal for this experiment is to demonstrate the feasibility of active structural control using both colocated and noncolocated measurements by means of successive control design and loop closing. More specifically, the colocated control loop was designed and closed first to provide good damping improvement over the frequency range of interest. The noncolocated controller was then designed with respect to a partially controlled structure to further improve the performance. Based on our approach, experimental closed-loop results have demonstrated significant performance improvement with excellent stability margins.

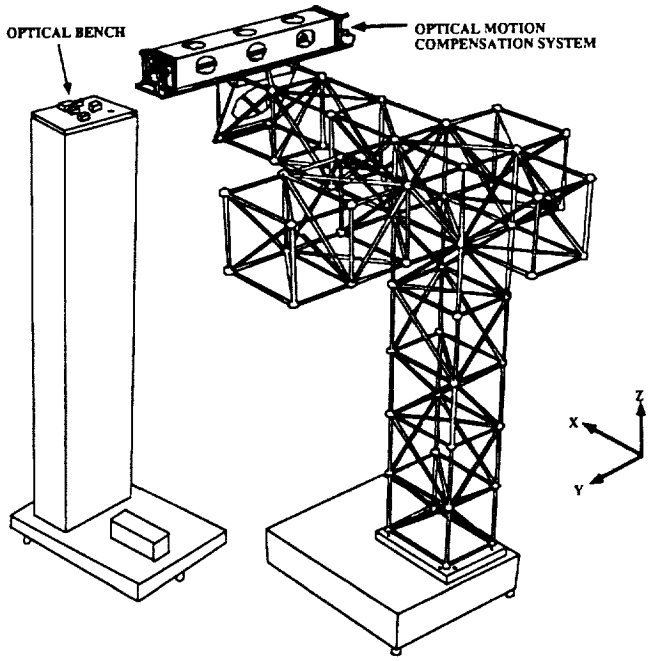

JPL's CSI Phase B Testbed

Motivation

Structural vibration control is necessary to satisfy the stringent pointing and shape requirements for future large precision flexible structures where the vibrations are introduced into the structure by both internal and external disturbances. There are various ways for structural control; for example, by isolation, by a passive damping method, or by active control. In a physical structure, it may be necessary to use a combination of isolators, passive dampers, actuators, and sensors to accomplish the desirable performance requirements. The effectiveness of all these methods will be decided by

1. the number of passive/active devices required or available,
2. the locations of these devices placed, and
3. the "optimal" strategy (control law) of these devices to be utilized.

In this study, only the approach of active control will be considered. The active control method typically involves designing a robust closed-loop feedback control law using a number of colocated and noncolocated sensors/actuators such that the resulting closed-loop system satisfies performance requirements while preserving stability.

Robust structural quieting control is critical to the success of future high precision large flexible structures.

Ways for structural quieting include:

- Passive Damping (viscous dampers, viscoelastic dampers, etc.),
- Active Damping (sensor/actuator colocation),
- Active Control (feedback control with colocated and/or noncolocated sensors and actuators),
- Isolation,
- Combination of the above.

Effectiveness of these methods will depend on:

- location(s) to be applied (placement problem), and
- the optimal strategy to be utilized (control problem).

Optimal Active Member Placement

For this experiment, only the piezoelectric active members will be considered as the actuation device. Since only one active member will be involved, an exhaustive search was conducted for the placement of the active member. This is feasible since there are only 186 candidate locations on the truss structure. Therefore, an $\mathcal{H}_2$ optimization problem was performed for each of the candidate locations. It is found that the element location # 133 (between grid 111 and 211) is the optimal location.

Note that the weighting function W_p is used to emphasize the frequency range where the performance will be optimized. W_u is the weighting function for the actuator signals which not only penalizes the control energy but also indicates the desired spectral content in actuator signals. This is due to the fact that any physical actuation device can only provide finite control energy, which is usually described in terms of saturation level (magnitude) and finite bandwidth.

The general optimal active member placement problem can be posed as an $\mathcal{H}_2$ optimization problem:

$$\min_{B_a \in \mathcal{B}_A} \min_{K \in \mathcal{K}} \|\mathcal{F}_l(P(s;B_a),K)\|_2$$

where

$$P(s;B_a) = \left[\begin{array}{c|c} P_{11} & P_{12} \\ \hline P_{21} & P_{22} \end{array}\right] = \left[\begin{array}{cc|c} W_p G_{pd} W_d & 0 & W_p G_p u(s;B_a) \\ 0 & 0 & W_u \\ \hline G_{md} W_d & W_n & G_{mu}(s;B_a) \end{array}\right]$$

$$\mathcal{F}_l(P(s;B_a),K) = P_{11} + P_{12}K(I - P_{22}K)^{-1}P_{21}$$

W_p (W_u): weighting function for performance (actuator signals),

W_d (W_n): coloring filter for disturbances (sensor noises),

G_{pd} (G_{md}): transfer matrix from disturbances to performance (measurements),

G_{pu} (G_{mu}): transfer matrix from actuators to performance (measurements),

$\mathcal{K} \triangleq \{ K$: any stabilizing feedback controller $\}$

$\mathcal{B}_A \triangleq \{(b_{i_1}, b_{i_2}, \ldots, b_{i_{n_a}}) : i_1, i_2, \ldots, i_{n_a} \in \mathcal{N}_A,\ i_j \neq i_k,\ \forall\, j,k = 1,2,\ldots,n_a\ (j \neq k)\ \}$

$\mathcal{N}_A \triangleq \{1, 2, \ldots, N_a\}$ (N_a is the total number of candidate locations).

Colocated and Noncolocated Structural Control Loops

The single active member placement study resulted in one active member placed at location 133 (between grid 111 and 211) to serve as the actuation device. There are two colocated measurements on the active member (internal displacement and force measurement) which are available for the design of colocated control. To simplify the design while preserving the interest of optical compensation control, the noncolocated measurement is chosen to be the μg. accelerometers. A μg accelerometer mounted at the tip of trolley in the Y direction was used to derive the model to facilitate the noncolocated feedback control system design. In addition, a suspended proof-mass shaker is used as an external disturbance input. The shaker injects an excitation force into grid point 412 via a stinger along the diagonal direction on the X-Y plane.

Our specific approach for the successive loop closing is to design the colocated control first. The noncolocated controller is then designed with respect to a partially controlled structure to further improve performance. Note that our colocated controller is implemented using the analog circuits. However, the noncolocated controller will be implemented digitally in a HUGH 9000 real-time controller [3].

It is our objective to demonstrate that using this approach, significant performance improvement can be achieved while providing excellent stability margins. Specifically for this experiment, the noncolocated measurement will also be used as the performance variable and the level of disturbance rejection from 3 to 13 Hertz will be used as the performance measure.

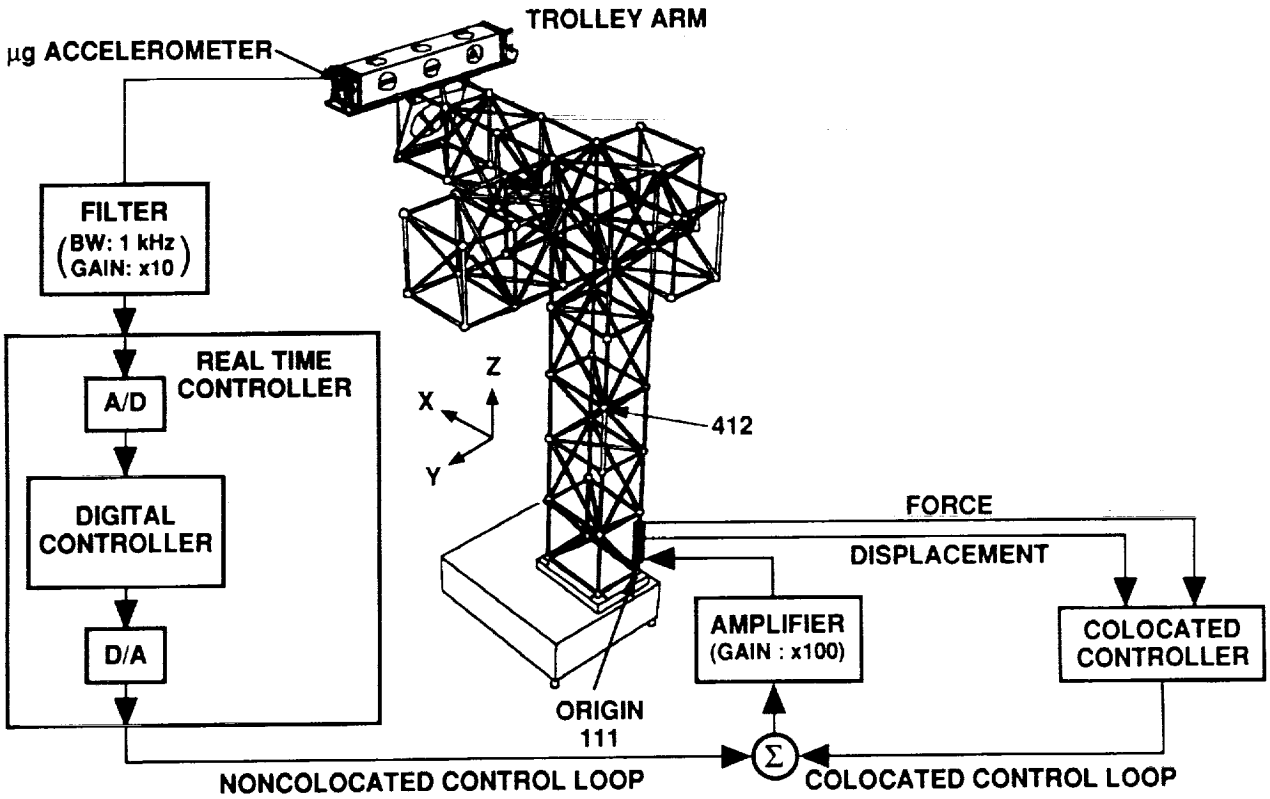

Colocated Control Design Using Impedance Matching

The impedance, defined as the ratio of velocity over force, of an active member is essentially reactive (like a spring). To introduce damping into a host structure in which the active member is embedded, two criteria must be met. First, the phase angle of the active member's impedance should be decreased from 90° (spring) to approximately 0° (viscous damper). Secondly, the magnitude of the active member's impedance should be increased (softening the strut) as to approximately match that of the rest of the host structure [4]. However, the static stiffness of the active member should be preserved so that it may still function as a stiff supporting strut.

For this experiment, only the colocated force measurement was used in designing the colocated controller. It is known that introducing constant colocated force feedback around an active member reduces its effective stiffness [5]. It does not, however, affect the phase angle of the active member's impedance. To reduce the phase angle, a Foster-form filter with a -4 db/octave roll-off was introduced in the force feedback loop which results in a phase lag of 60°. This phase lag dropped the phase angle of the active member's impedance. As a result, the two criteria for impedance matching are both met. Note that the force sensor used in this experiment is a piezo-type load cell which can measure dynamic loads only. Thus, the force feedback did not diminish the high static stiffness of the active member.

Experimental results show that approximately a factor of 10 in performance improvement (disturbance rejection) was achieved, and significant damping was introduced in the first 3 structural modes.

Comparison of Open-Loop and Closed-Loop Frequency Response (from disturbance shaker load cell to μg accelerometer at 752Y)

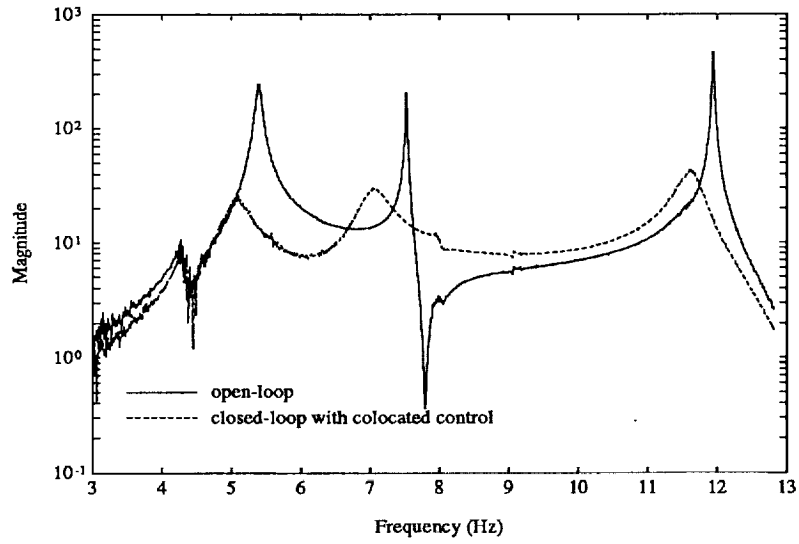

System Identification

With the colocated force feedback loop closed, system identification experiments were conducted where the high resolution, input-output frequency response data corresponding to the 2 inputs (active member voltage input and disturbance shaker load cell) and 1 output (μg accelerometer at grid 752Y) were measured.

To identify a linear state-space model corresponding to the measured data, two key steps are involved in our approach. The technique of Chebyshev polynomial curve fitting [6] is used first to derive a stable state-space model which qualitatively fits well to the measured frequency response data. This model is then refined using a linear least-squares curve fitting technique [7] to update the state-space matrices iteratively. As a result, a 2-input, 1-output, 26-state state-space model was identified for the measured data below 30 Hertz. This model includes 12 complex modes (see table below) and 2 real poles (14.3225 & 71.9783 radian/second). Comparison between the measured data (solid line) and frequency responses of the identified model (dashed line) shows an excellent match in both magnitude and phase. This model will serve as the nominal model in designing the noncolocated control system using the $\mathcal{H}_\infty$ synthesis technique.

Identified Modal Frequency and Damping

Mode No.	Frequency (Hz)	Damping (%)	Mode No.	Frequency (Hz)	Damping (%)
1	4.3490	0.4311	7	19.4532	0.1429
2	5.0974	3.7001	8	20.0208	0.4657
3	7.0189	3.8321	9	21.6467	0.5338
4	11.6512	1.4961	10	25.1737	0.4463
5	17.0516	1.1378	11	27.3367	0.0355
6	19.0184	1.8772	12	27.3569	0.0271

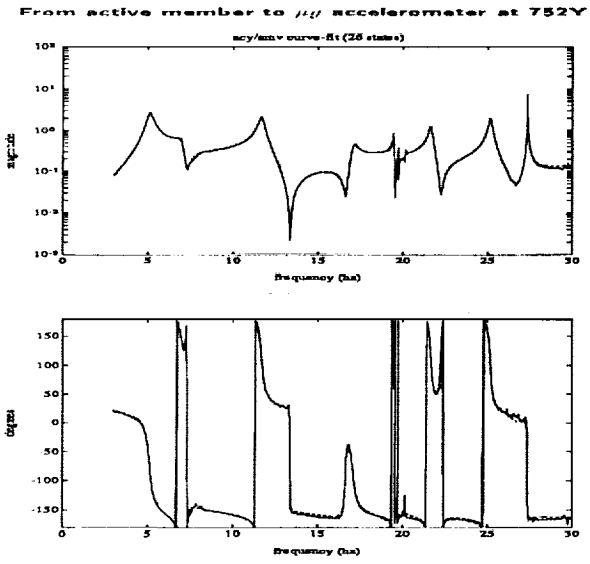

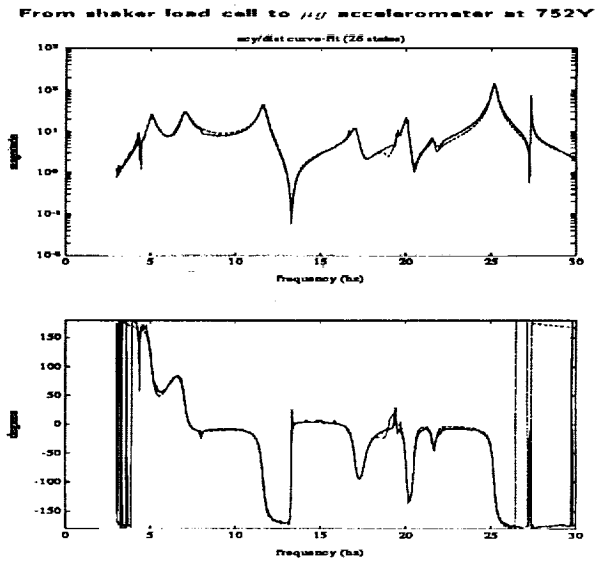

Robust Control System Design – $\mathcal{H}_\infty$ Synthesis

The noncolocated controller has been designed using the $\mathcal{H}_\infty$-synthesis approach [8,9]. Two types of uncertainty are used, multiplicative and additive. W_{mult} and W_{add} are frequency dependent uncertainty weights. The larger additive weighting, W_{add}, at frequencies greater than 15 Hz reflects the fact that the system is more uncertain at higher frequencies. A constant W_{mult} is used to capture the effects of mode shape errors [10]. W_{delay} is a Pade approximation of one sample delay — in this case $\frac{1}{1000}$ seconds. W_{perf} weights the acceleration output which has larger magnitude from 3 to 13 Hertz to emphasize the frequency range of primary control interest. W_{act} is used to penalize the active member voltage input signal at both higher and lower frequencies to avoid the amplification of high frequency noise and to prevent the controller from responding to accelerometer drift which may cause the saturation problem. W_{noise} reflected the sensor noise problem which also penalizes the lower frequencies more to account for the the same accelerometer drift problem. The disturbance weight, W_{dist}, rolls off sharply after 15 Hz as the disturbance is expected to be band limited to this range.

The associated control design problem can easily be rearranged to form the standard $\mathcal{H}_\infty$ synthesis block diagram as shown below. All of the weighting functions, and the nominal model G derived from system identification, have been absorbed into the interconnection structure P. The $\mathcal{H}_\infty$ synthesis problem now becomes to find K such that the closed-loop transfer function from the inputs (shaker disturbance & sensor noise) to the outputs (acceleration & actuator) is internally stable and has a minimum $\mathcal{H}_\infty$ norm for all possible Δ, $\|\Delta\| \leq 1$.

Block Diagram for Control System Design

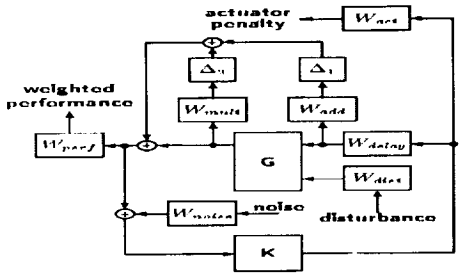

Weighting Functions

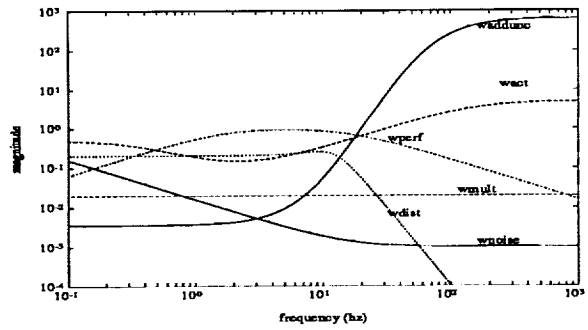

Generic Interconnection Structure for Robust Control System Design

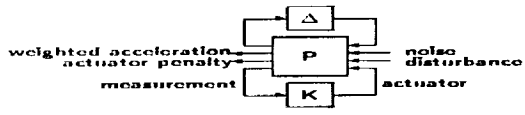

$\mathcal{H}_\infty$ Synthesis

$$Min_{K \in \mathcal{H}_\infty} \|T_{yu}(K, \Delta)\|_\infty$$

Subject to $\|\Delta\| \leq 1$

$\mathcal{H}_\infty$ Design – Results

A stabilizing controller using the noncolocated measurement was obtained using the $\mathcal{H}_\infty$ synthesis methodology. The bode plots of the loop gain show that the higher frequencies (> 15 Hertz) are gain-stabilized and the lower frequencies (< 15 Hertz) are phase-stabilized. A further examination of the corresponding Nyquist plot indicates that approximately 6.5 db of gain margin and 72° of phase margin were achieved by the closed-loop system. Therefore, this closed-loop system with both colocated and noncolocated control is robustly stable.

A comparison of the actual, predicted, and nominal disturbance rejection frequency response is also plotted which shows the predicted and the nominal performance are reasonably close to the experimental performance. This observation reassures us that the system identification and the digital implementation in our design process were carried out properly.

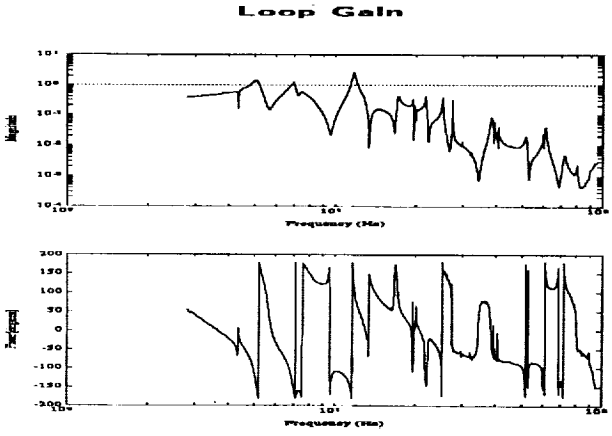

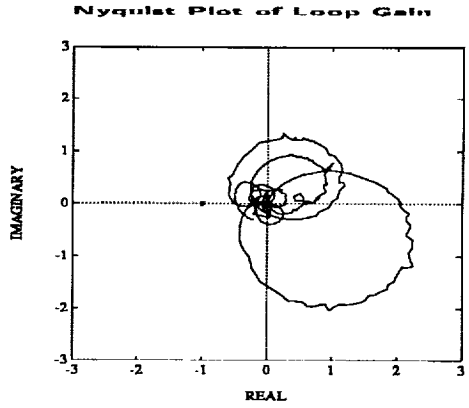

Experimental, Predicted, and Nominal Performance

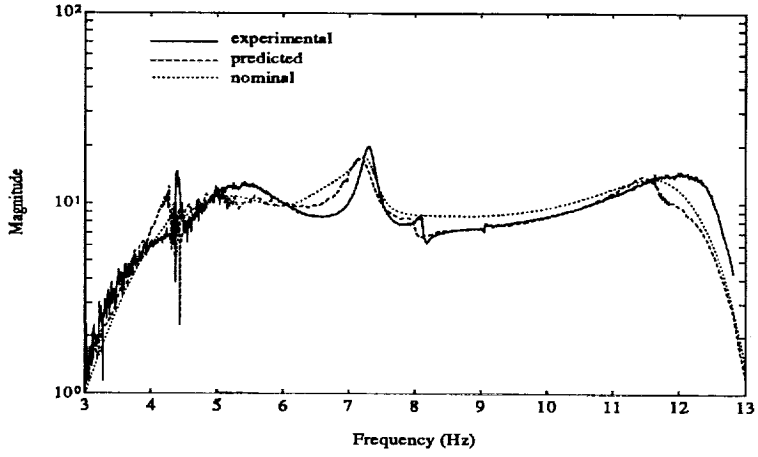

Performance (Disturbance Rejection) Comparison

The effect of feedback control on performance is shown below. Frequency responses from disturbance shaker load cell to μg accelerometer at 752Y are plotted for

1. the open-loop,
2. closed-loop with colocated control only, and
3. closed-loop with both colocated and noncolocated control.

Experimental results show that on the average, the colocated control alone achieves a factor of 10 improvement in performance (disturbance rejection) over the uncontrolled structure (open-loop). However, by means of closing the colocated and noncolocated control loop successively, a factor of 20 improvement has been achieved.

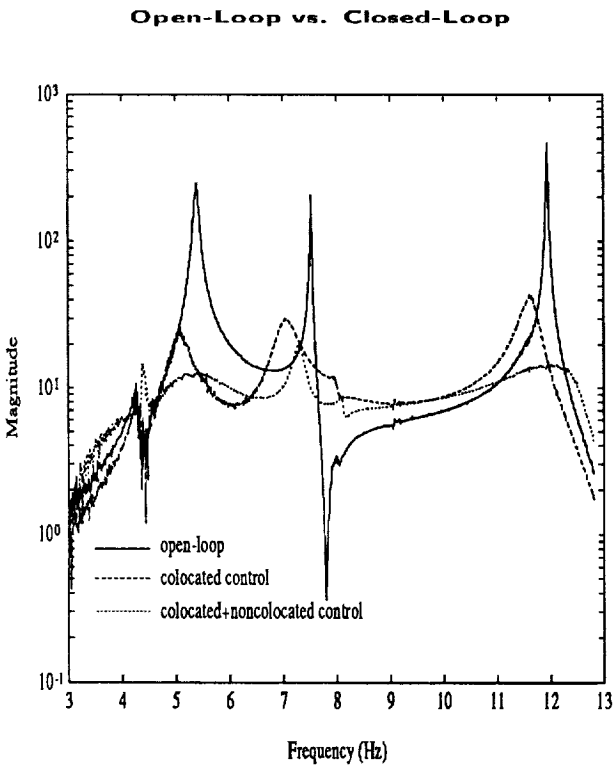

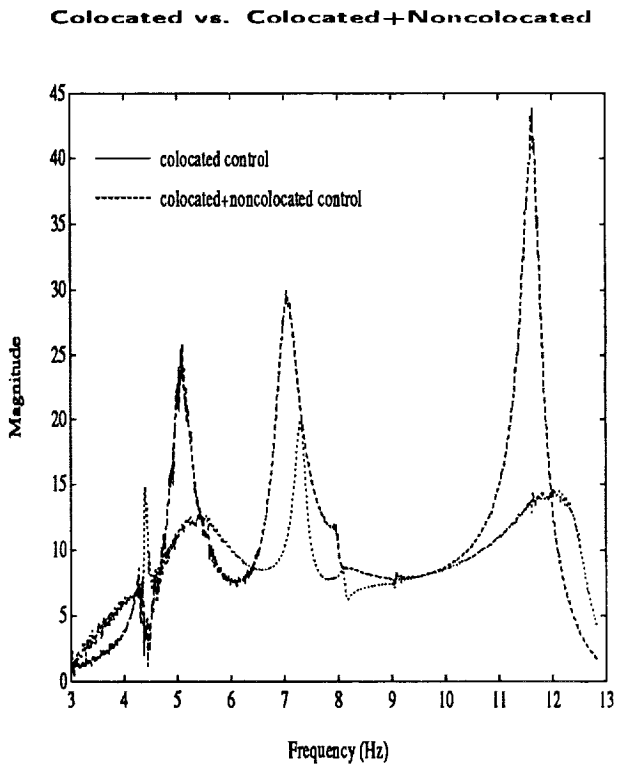

Conclusions and Future Work

In this study, the feasibility of the successive colocated and noncolocated control design and loop closing has been successfully demonstrated. It is shown that more than an order of magnitude performance improvement can be achieved easily with only one properly placed active member. It is our immediate plan to extend the noncolocated control bandwidth to the higher frequency region. This certainly will pose a much greater challenge to system identification and control design since more structural dynamics will be involved.

A parallel study is currently underway on the simultaneous design and closing of both colocated and noncolocated feedback control loops. It will be very interesting to compare the stability and performance aspect of these two (successive and simultaneous) approaches.

Our study of the passive damper placement and tuning problem [11] has shown that the dampers can be used very effectively to damp out modes in the frequency region which might be troublesome for the active control design. It is our goal that all these studies will eventually lead to a feasible solution to the multilayer structural control problem where multiple active and passive devices will be involved.

Acknowledgments

The research described in this paper was carried out by the Jet Propulsion Laboratory, California Institute of Technology, under contract with the National Aeronautics and Space Administration.

References

1. Laskin, R.A., and San Martin, M., "Control/Structure System Design of a Spaceborne Optical Interferometer," Proceedings of the AAS/AIAA Astrodynamics Specialist Conference, Stowe VT, 1989.

2. O'Neal, M., Eldred, D., Liu, D., and Redding, D., "Experimental Verification of Nanometer Level Optical Pathlength Control on a Flexible Structure," 14th Annual AAS Guidance and Control Conference, Keystone, CO, February, 1991.

3. Fanson, J.L., Briggs, H.C., Chu, C.C., Lurie, B.J., Smith, R.S., Eldred, D.B., and Liu, D. "JPL CSI Phase–0 Experiment Results and Real Time Control Computer," 4th NASA/DoD Control/Structures Interaction Technology Conference, Orlando, FL, Nov. 5–7, 1990.

4. Lurie, B.J., Sirlin, S.W., O'Brien, J.F., and Fanson, J.L., "The Dial-a-Strut Controller for Structural Damping," ADPA/AIAA/ASME/SPIE Conference on Active Materials and Adaptive Structures, Alexandria, VA, November 5–8, 1991.

5. Fanson, J.L., Lurie, B.J., O'Brien, J.F., Chu, C.C., and Smith, R.S., "System Identification and Control of the JPL Active Structure," 32nd AIAA/ASME/ASCE/AHS Structures, Structural Dynamics, and Material Conference, Baltimore, MD, April 8–10, 1991.

6. Dailey, R.L. and Lukich, M.S., "MIMO Transfer Function Curve Fitting Using Chebyshev Polynomials," SIAM 35^{th} Anniv. Meeting, Denver, CO, 1987.

7. Smith, R.S., *Procedures for the Identification of Precision Truss*, JPL D–7791, 1990.

8. Doyle, J.C. and Chu, C.C., *Robust Control of Multivariable and Large Scale Systems*, Final Technical Report for AFOSR, Contract No. F49620-84-C-0088, March, 1986.

9. Doyle, J.C., Glover, K., Kharagonekar, P., and Francis, B.A., "State-Space Solutions to Standard $\mathcal{H}_2$ and $\mathcal{H}_\infty$ Control Problems," IEEE Transactions on Automatic Control, Vol. 34, No. 8, 1989.

10. Balas, G.J., *Robust Control of Flexible Structures Theory and Experiments*, Ph.D. Thesis, California Institute of Technology, 1989.

11. Chu, C.C., Milman, M.H., and Kissil, A., "Optimal Passive Damper Placement and Tuning Using Ritz Model Reduction Method," ADPA/AIAA/ASME/SPIE Conference on Active Materials and Adaptive Structures, Alexandria, VA, November 5–8, 1991.